

# Comparative chemistry of diffuse clouds

## I. C<sub>2</sub>H and C<sub>3</sub>H<sub>2</sub>

R. Lucas<sup>1</sup> and H.S. Liszt<sup>2</sup>

<sup>1</sup> Institut de Radioastronomie Millimétrique, 300 Rue de la Piscine, 8406 Saint Martin d'Hères, France

<sup>2</sup> National Radio Astronomy Observatory, 520 Edgemont Road, Charlottesville, VA 22903-2475, USA

Received 8 March 2000 / Accepted 17 April 2000

**Abstract.** Using the Plateau de Bure interferometer, we searched for  $\lambda$ 3mm absorption lines of C<sub>2</sub>H, C<sub>3</sub>H<sub>2</sub>, C<sub>3</sub>H, and C<sub>4</sub>H from the diffuse and very marginally translucent clouds which lie toward a sample of compact extragalactic mm-wave continuum sources. The C<sub>2</sub>H survey in particular is nearly the equivalent of our earlier, exhaustive study of HCO<sup>+</sup> absorption, albeit with lower signal/noise.

C<sub>2</sub>H lines are found corresponding to all components detected in HCO<sup>+</sup> which places C<sub>2</sub>H in a small group of the most ubiquitous molecules we have studied – OH, HCO<sup>+</sup> and, from this work, C<sub>2</sub>H and C<sub>3</sub>H<sub>2</sub>. But the relationship between N(C<sub>2</sub>H) and N(HCO<sup>+</sup>) is highly non-linear, as seems to be the case for all species beside OH. N(C<sub>2</sub>H)/N(HCO<sup>+</sup>) is actually relatively high at small N(HCO<sup>+</sup>), 20–40, and declines at higher column density despite a typically steep increase of N(C<sub>2</sub>H) around N(HCO<sup>+</sup>)  $\approx 10^{12}$  cm<sup>-2</sup>. On the whole we find a mean over all features of  $\langle N(\text{C}_2\text{H})/N(\text{HCO}^+) \rangle = 14.5 \pm 6.7$  or  $\langle N(\text{C}_2\text{H})/N(\text{H}_2) \rangle \approx 2.9 \pm 1.3 \times 10^{-8}$ .

By contrast, C<sub>2</sub>H and ortho cyclic-C<sub>3</sub>H<sub>2</sub> vary in nearly fixed proportion,  $\langle N(\text{C}_2\text{H})/N(\text{C}_3\text{H}_2\text{-o}) \rangle = 27.7 \pm 8.0$ , leading to a total C<sub>3</sub>H<sub>2</sub> abundance  $N(\text{C}_3\text{H}_2)/N(\text{H}_2) \approx 1.4 \pm 0.7 \times 10^{-9}$  and  $\langle N(\text{C}_3\text{H}_2)/N(\text{HCO}^+) \rangle \approx 0.7$ . Our observations of the high-lying C<sub>4</sub>H lines at 95 GHz do not place sensitive limits on N(C<sub>4</sub>H)/N(HCO<sup>+</sup>). The C<sub>3</sub>H data are somewhat more restrictive, and we find  $N(\text{C}_3\text{H})/N(\text{HCO}^+) < 0.065$  in one direction but more generally we have only that  $N(\text{C}_3\text{H})/N(\text{HCO}^+) < 4$ . The linewidths of C<sub>2</sub>H, C<sub>3</sub>H<sub>2</sub>, and HCO<sup>+</sup> are sensibly identical.

In comparing the abundances of many simple species in diffuse, translucent, and dark gas, we see that the relative abundances of OH, HCO<sup>+</sup>, CH, and C<sub>2</sub>H are relatively constant, but those of C<sub>3</sub>H<sub>2</sub> and C<sub>3</sub>H are noticeably larger in TMC-1.

**Key words:** ISM: abundances – ISM: clouds – ISM: molecules – ISM: structure – radio lines: ISM

### 1. Introduction

The simple hydrocarbons CH (Swings & Rosenfeld 1937) and CH<sup>+</sup> (Douglas & Herzberg 1941) were among the first

molecules identified in the interstellar medium, in what have come to be known as diffuse clouds. Although Swings and Rosenfeld noted that CH, OH, NH, CN, and C<sub>2</sub> were obvious candidates for identification, the program of finding all of these simple species was not completed for 55 years (Meyer & Roth 1991). Indeed, the notion of a separately identifiable molecular component of the interstellar medium was slow to develop and we are actually still discovering, and being surprised by, the ubiquity of molecules in the diffuse ISM.

One of these surprises was the widespread presence (Matthews & Irvine 1985; Cox et al. 1988) of the cyclic ring species C<sub>3</sub>H<sub>2</sub> (Thaddeus et al. 1985b; Vrtilik et al. 1987); having 5 atoms, and forming (almost certainly) as the recombination or dissociation product of a even larger species (at the very least, from C<sub>3</sub>H<sub>3</sub><sup>+</sup> + e → C<sub>3</sub>H<sub>2</sub> + H) we are reminded once again that the actual complexity of diffuse cloud chemistry is viewed only very dimly in those species which we have yet surveyed.

In our work, we have shown that many species viewed through the technique of mm-wave absorption pioneered by (Marscher et al. 1991) are present with abundances remarkably like those which occur in dense dark clouds (Lucas & Liszt 1993, 1994, 1996): examples are HCO<sup>+</sup>, HCN, C<sub>2</sub>H and species familiar from earlier work like H<sub>2</sub>CO (Liszt & Lucas 1995) and CN. Although the high abundances of such species in diffuse gas are not understood, they imply that some of classical problems of interstellar chemistry must be recast. For instance, if the observed, relatively constant abundance of HCO<sup>+</sup> is inserted into very standard models of diffuse gas undergoing the HI-H<sub>2</sub> transition, it follows with no other assumptions that the observed variation of N(CO) and N(H<sub>2</sub>) can be explained over the entire range  $10^{12}$  cm<sup>-2</sup>  $\leq$  N(CO)  $\leq$   $3 \times 10^{16}$  cm<sup>-2</sup> simply by the reaction HCO<sup>+</sup> + e → CO + H (Liszt & Lucas 2000). In like fashion, with high demonstrated abundances of HCN, C<sub>2</sub>H or C<sub>3</sub>H<sub>2</sub> need one really worry very much about making CH, CN, C<sub>2</sub>, or C<sub>3</sub>?

Here we report the results of a survey of mm-wave absorption from various hydrocarbons – C<sub>2</sub>H, ortho- and para-cyclic-C<sub>3</sub>H<sub>2</sub>, C<sub>3</sub>H, and C<sub>4</sub>H – which occur in the clouds occulting our usual sample of compact extragalactic mm-wave continuum sources. Most of the work consists of a very large survey of the 87.3 GHz C<sub>2</sub>H N=0-1 lines which fully complements our

Send offprint requests to: H.S. Liszt (hliszt@nrao.edu)

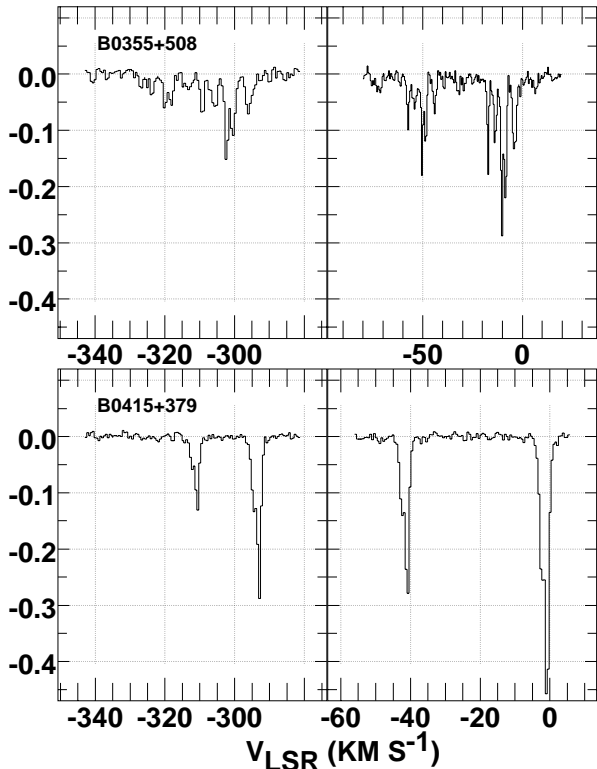


**Fig. 1.**  $C_2H$  absorption spectra for two sources, showing four hyperfine components. The velocity scale is relative to the frequency of the strongest component; in the upper figure, the velocity scale differs between the right and left frames.

earlier, analogous report on  $HCO^+$  (Lucas & Liszt 1996). Although it is  $C_3H_2$  which is understood to be so ubiquitous, and although it was only several years after its discovery that  $C_2H$  was found in any molecular clouds except the densest GMC's (Wootten et al. 1980),  $C_2H$  emission is widespread over the entire inner galactic plane (Liszt 1995).  $C_2H$  is more abundant than  $C_3H_2$  by roughly a factor thirty, and is more favorably observed despite its lower dipole moment (0.8 vs. 3.27 Debye). The abundances of  $C_2H$  and  $C_3H_2$  increase in fixed proportion with respect to each other, and they vary differently with respect to the exemplars of other chemical groupings, notably  $HCO^+$  and  $OH$ , or  $HCN$ ,  $HNC$ , and  $CN$ . The other chemical groups will be the subject of forthcoming papers in this series, beginning with  $HCN$ ,  $HNC$ , and  $CN$ . A recent, more comprehensive summary of profiles in  $OH$  and  $HCO^+$  (*cf.* Liszt & Lucas (1996)) which might be considered Paper 0 in this series, will appear shortly (Liszt & Lucas 2000).

The observations and manner of data-taking are discussed in Sect. 2. Sect. 3 is a presentation of the observational results and Sect. 4 is a brief discussion of molecular origins.

## 2. Observations

### 2.1. $C_2H$

The bulk of the work reported here is a survey of 87 GHz  $N=0-1$   $C_2H$  absorption meant to complement

**Table 1.** Background Source and profile rms

Source	l °	b °	$\sigma_{l/c}$ $C_2H$	$\sigma_{l/c}$ $C_3H_2-(o)$
B0212+735	128.93	11.96	0.031	0.022
B0224+671	132.12	6.23	0.016	
B0316+413	150.58	-13.26	0.008	
B0355+508	150.38	-1.60	0.011	0.022
B0415+379	161.68	-8.82	0.005	0.004
B0420-014	195.29	-33.14	0.009	
B0528+134	191.37	-11.01	0.020	0.020
B0552+398	171.65	7.29	0.011	
B0607-157	222.61	-16.18	0.007	
B0736+017	216.99	11.38	0.017	
B0923+392	183.71	46.16	0.006	
B0954+658	145.75	43.13	0.018	
B1055+018	251.51	52.77	0.010	
B1226+023	289.95	64.36	0.002	
B1253-055	305.11	57.06	0.004	
B1334-127	320.03	48.37	0.005	
B1641+399	63.45	40.95	0.012	
B1730-130	12.03	10.81	0.006	0.004
B1741-038	21.59	13.12	0.008	
B1749+096	34.92	17.64	0.008	
B1823+568	85.74	26.08	0.010	
B1908-201	16.88	-13.22	0.009	
B1923+738	105.63	23.55	0.006	
B1954+513	85.30	11.76	0.024	
B2037+511	88.81	6.04	0.006	
B2145+067	63.66	-34.07	0.006	
B2200+420	92.13	-10.40	0.059	0.005
B2251+158	86.11	-38.18	0.013	0.008

our earlier, approximately flux-limited survey of  $HCO^+$  (Lucas & Liszt 1996). The 87 GHz spectrum of  $C_2H$  (Tucker et al. 1974; Gottlieb et al. 1983a) has 6 hyperfine components of relative LTE strengths 43:417:208:208:83:43 in the spectral region from 87.28416 to 87.44651 GHz. The strongest line at 87.316924 GHz was taken as the zero-velocity rest frequency for our work. We typically observed the strongest four components as shown in Fig. 1.

Table 1 shows the list of background sources observed, their galactic coordinates and the rms error in the line/continuum ratio, which is also the rms error in optical depth in the optically thin limit. In Table A1 of the Appendix we show the results of gaussian fitting, done simultaneously to whichever subset of the hyperfine structure was actually observed. The optical depth quoted at line center is for the strongest component (but results from a fit to multiple components assumed to appear in the LTE ratio) and the integrated optical depth is the sum over all six hyperfine components, which we derive by a simple scaling to account for that (smaller) fraction of the line which was not actually observed. In the limit of no collisional excitation above the black body background (all excitation temperatures = 2.73 K), the optical depth integrals are related to the total column density *via*  $N(C_2H) = 1.70 N_0 = 2.71 \times 10^{13} \text{ cm}^{-2} \int \tau dv$ , where we have taken the permanent dipole moment as 0.8 Debye. Com-

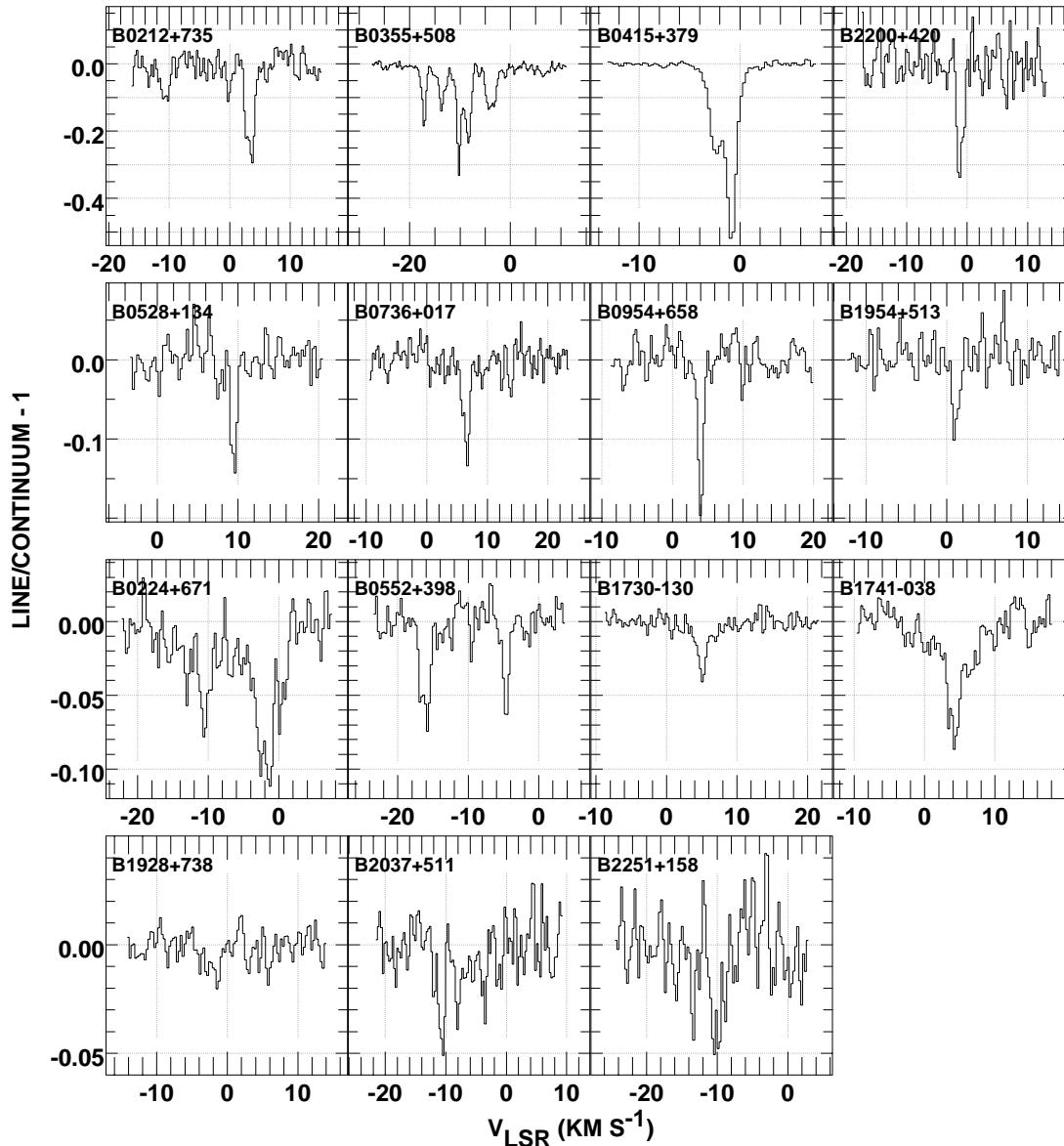


Fig. 2. Digest of detected  $C_2H$  87.3GHz absorption profiles seen at the Plateau de Bure Interferometer for the strongest hyperfine component of the  $N=0-1$  transition. The channel spacing is 78kHz and the resolution is 140 kHz ( $0.48 \text{ km s}^{-1}$ )

parison with the analogous expressions for  $C_3H$  and  $C_4H$  in Sects. 2.3 and 2.4 will show why our limits on those species are poor: the correction for the partition function is much larger.

The data were taken at various times between mid-1993 and mid-1997. In all cases the spectral channel separation was 78.1 kHz ( $0.268 \text{ km s}^{-1}$  at the strongest hyperfine component). The actual resolution of the data shown here is lower, however, 140 kHz ( $0.481 \text{ km s}^{-1}$ ).

## 2.2. Cyclic $C_3H_2$

We observed  $1_{01} - 2_{12}$  absorption from ortho cyclic- $C_3H_2$  at 85338.91GHz and  $1_{11} - 2_{02}$  absorption from para cyclic  $C_3H_2$  at 82093.56 GHz, both of which arise from levels within about 2 K of the ground state (Vrtilik et al. 1987). The ratio of statis-

tical weights is ortho:para = 3:1. The spectra were taken over the period 1994-1997 with the usual 140 kHz- wide channels sampled at 78.1 kHz intervals, leading to a velocity resolutions of 0.285 and  $0.274 \text{ km s}^{-1}$  for the para and ortho lines. For B2200+420, we also took a 1997 spectrum with two times narrower channels, as shown in Fig. 3. The 7 sources observed are noted in Table 1, where the rms noise in baseline line/continuum ratio for the ortho-species is given in the last column.

The dipole moment of  $C_3H_2$  is 3.27 Debye (Lovas et al. 1992). The column density and integrated optical depth (for the transitions observed here) are related by  $N(C_3H_2-(o)) = 4.36 \times 10^{12} \text{ cm}^{-2} \int \tau dv$ , or  $N(C_3H_2-(p)) = 5.47 \times 10^{12} \text{ cm}^{-2} \int \tau dv$ , in the limit of no collisional excitation above the cosmic blackbody background.

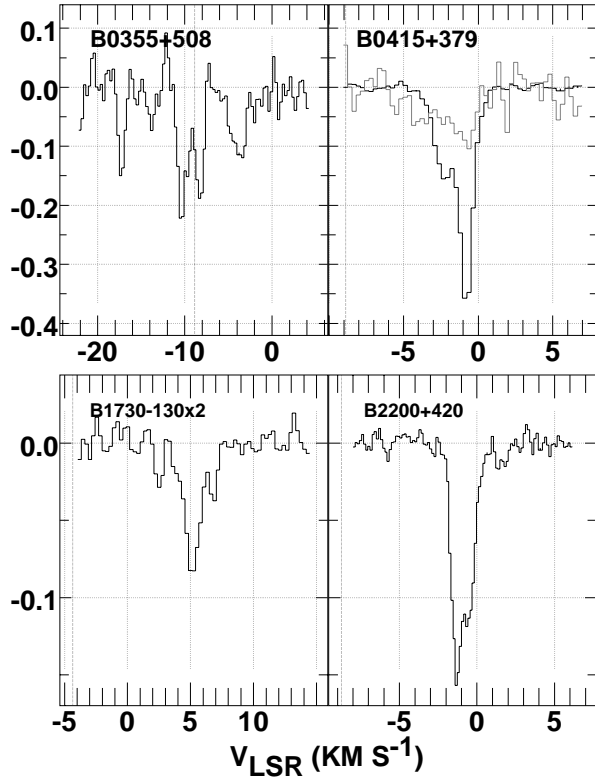


**Fig. 3.**  $C_3H_2$ -(o) absorption spectra for four sources. The profile for B1730-130 has been multiplied by a factor two. Toward B0415+379 at upper right, the profile for  $C_3H_2$ -(p) is shown shaded.

The products of gaussian fitting of the  $C_3H_2$ -(o) profiles are given in Table A2 of the Appendix.

### 2.3. Linear $C_3H$

We observed the  $J=7/2-9/2$  transitions of linear  $C_3H$  near 97995.45 GHz, *i.e.* the two hyperfine components separated by 0.75 MHz (Gottlieb et al. 1986). For a dipole moment of 3.1 Debye, using the partition function of Thaddeus et al. (1985a), we find  $N(C_3H) = 44.7 N_{7/2} = 1.61 \times 10^{14} \text{ cm}^{-2} \int \tau_{7/2-9/2} dv$  in the limit of no excitation above the cosmic microwave background. For the line of sight toward B0415+379, we find  $N(C_3H) < 0.065 N(HCO^+)$  at the  $2\sigma$  level, while for B0355+508, B0528+134, B1730-130, and B2251+158, we have coincidentally similar but much poorer limits  $N(C_3H) \lesssim 4 N(HCO^+)$ .

### 2.4. $C_4H$

We observed one of the paired spin doublets of the  $J=9-10$  transition of  $C_4H$  at 95188.94 GHz (Gottlieb et al. 1983b). For a dipole moment of 0.9 Debye, and in the limit of no collisional excitation, it follows that  $N(C_4H) = 1545 N_9 = 7.25 \times 10^{16} \text{ cm}^{-2} \int \tau dv$  where the integral is taken over one spin doublet. This leads to rather poor limits, the best of which is  $N(C_4H) < 666 N(HCO^+)$  toward B0415+379 ( $2\sigma$ ). For B0355+508, B0528+134, B1730-130, and B2251+158, we have only that  $N(C_4H) < 1500-2200 N(HCO^+)$ . It is straightforward to show

that much better limits on the abundance of  $C_4H$  would be available for the 10 GHz transitions from lower-lying transitions, in cases of weak collisional excitation.

## 3. Systematics

### 3.1. $C_2H$

The individual  $C_2H$  spectra are displayed in Figs. 1 and 2. There were no detectable anomalies in the ratios of the hyperfine lines and the line parameters in Table A1 derive from a simultaneous fitting of several hyperfine components under the assumption of LTE line ratios.

In our earlier work (Lucas & Liszt 1997) the systematic variation of  $C_2H$  and  $HCO^+$  was not readily apparent, owing to the small number of lines of sight, and it appeared that  $C_2H$  and  $HCO^+$  were largely decoupled. Fig. 4 at bottom shows perhaps the most important results of this work: that  $C_2H$  is as widespread as  $HCO^+$ , that the  $C_2H/HCO^+$  ratio actually is fairly high (in the mean) at low column density where values as high as 35 are seen at  $N(HCO^+) = 2 \times 10^{11} \text{ cm}^{-2}$ , and that the column densities of  $C_2H$  and  $HCO^+$  are strongly coupled.

For the  $C_2H/HCO^+$  abundance ratio we calculate an unweighted mean over the individual components of  $14.5 \pm 6.7$ , implying  $N(C_2H)/N(H_2) \approx 2.9 \pm 1.3 \times 10^{-8}$  assuming  $N(HCO^+)/N(H_2) = 2 \times 10^{-9}$  (Lucas & Liszt 1996; Liszt & Lucas 1996, 2000).

### 3.2. $C_3H_2$

Spectra of  $C_3H_2$ -(o) toward 4 sources are shown in Fig. 3 and Table A2 lists the decomposition products of all detected lines. The detection toward B0528+134 is rather marginal. The column densities of  $C_3H_2$  and  $C_2H$  are strongly and nearly linearly related, as shown in Fig. 4 at top. Given the long-known ubiquity of  $C_3H_2$ , the strong correlation between  $C_3H_2$  and  $C_2H$  reinforces the notion that  $C_2H$  is ubiquitous as well. The mean abundance ratio weighted by the variance is  $\langle C_2H/C_3H_2\text{-(o)} \rangle = 27.7 \pm 8$ , and for the abundance we have  $N(C_3H_2)/N(H_2) = (4/3) N(C_3H_2\text{-(o)})/N(H_2) = 1.4 \pm 0.7 \times 10^{-9}$ .

#### 3.2.1. The ortho/para ratio in $C_3H_2$

We detected para- $C_3H_2$  toward B0355, B0415, and B1730 finding para/ortho ratios of  $0.29 \pm 0.060$ ,  $0.56 \pm 0.083$ , and  $0.243 \pm 0.060$  respectively. The weighted mean of these is (coincidentally) 0.33. The line of para- $C_3H_2$  toward B0415 is shown in Fig. 3.

### 3.3. $C_4H$ and linear $C_3H$

For the line of sight toward B0415+379, we find  $N(C_3H) < 8.7 \times 10^{11} \text{ cm}^{-2}$  at the  $2\sigma$  level, or  $N(C_3H) < 0.065 N(HCO^+)$ . For B0355+508, B0528+134, B1730-130, and B2251+158, we have coincidentally similar but much poorer limits  $N(C_3H) \lesssim 4 N(HCO^+)$ .

**Table 2.** Relative abundances  $10^8 \times N(\text{O})/N(\text{H}_2)$ 

Species	$\zeta$ Oph	This Work	TMC-1	BD-G
OH	10	7	30	10
CO	480		8000	41
HCO <sup>+</sup>	0.2	0.2	0.8	0.009
C <sup>+</sup>	26100			89100
C	700			720
C <sub>2</sub>	3.3			3.7
C <sub>3</sub>	< 0.012			$10^{-5}$
CH	5.4	1-2	2	3.9
CH <sup>+</sup>	6.3			0.006
C <sub>2</sub> H		1.6-4.2	7	0.4
C <sub>3</sub> H		< 0.02	0.05	
C <sub>3</sub> H <sub>2</sub>		0.07-0.21	3	
C <sub>4</sub> H			2.0	

This work:  $N(\text{C}_3\text{H}_2) = 4/3 \times N(\text{ortho-C}_3\text{H}_2)$ ; CH is our unpublished work and  $N(\text{OH}) = 35 \times N(\text{HCO}^+)$  (Liszt & Lucas 1996)

TMC-1: results from Ohishi et al. (1992)

$\zeta$  Oph:  $N(\text{C}^+)$  is from Cardelli et al. (1993)

BD-G: results from model  $\zeta$  Oph G of Van Dishoeck & Black (1986)

As noted in Sect. 2, the mm-wave lines of C<sub>4</sub>H are too high up the rotation ladder to derive good limits in the absence of substantial excitation. Our result that  $N(\text{C}_4\text{H}) < 1000\text{-}2000 N(\text{HCO}^+)$  is of little interest. C<sub>4</sub>H is better studied at  $\lambda 3\text{cm}$  than  $\lambda 3\text{mm}$ .

### 3.4. Linewidths and kinematics

A plot of the linewidths of C<sub>2</sub>H and HCO<sup>+</sup> shows a dominant linear relationship with some significant outliers. The outliers can all be attributed to weak or blended lines and we conclude that there is no statistically significant difference between the derived linewidths of these species.

Fig. 5 shows a comparison of C<sub>2</sub>H (histogram) and HCO<sup>+</sup> (shaded) profiles in three sources (see the figure caption for an explanation of scaling). The tendency for the C<sub>2</sub>H/HCO<sup>+</sup> ratio to be high in some weak lines is evident in the  $-11 \text{ km s}^{-1}$  gas toward B0212+735 and perhaps between the two components around  $-10 \text{ km s}^{-1}$  toward B0355+508, although the HCO<sup>+</sup> profile in this direction has somewhat higher resolution. Toward B1730-130 the HCO<sup>+</sup> may be narrower, but the baseline level in the C<sub>2</sub>H profile seems somewhat uncertain. Fig. 6 shows a comparison of the C<sub>2</sub>H toward B0415+379 with OH, H<sup>13</sup>CO<sup>+</sup> (because H<sup>12</sup>CO<sup>+</sup> is somewhat saturated) and C<sub>3</sub>H<sub>2</sub>. The best match for the C<sub>2</sub>H is actually with C<sub>3</sub>H<sub>2</sub>.

Clearly, there are no systematic differences between the kinematics of C<sub>2</sub>H and those of the other species.

## 4. Comparative chemistry of simple carbon chains and hydrocarbons

### 4.1. Comparison with some prior results for C<sub>3</sub>H<sub>2</sub>

C<sub>3</sub>H<sub>2</sub> was discovered in the interstellar medium along lines of sight lacking truly dark clouds (Matthews & Irvine 1985),

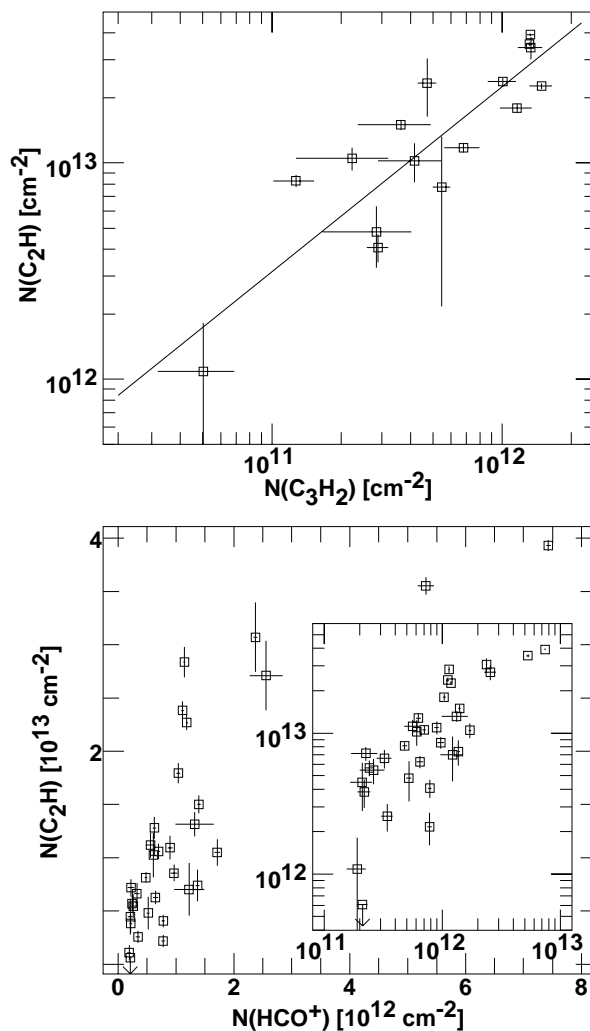


**Fig. 4.** Top: variation of C<sub>2</sub>H with C<sub>3</sub>H<sub>2</sub>: the regression line has a power law slope of  $0.86 \pm 0.13$ . Bottom:  $N(\text{C}_2\text{H})$  vs.  $N(\text{HCO}^+)$  on linear and (inset) log scales.

for instance toward Cas A. Cox et al. (1988) observed C<sub>3</sub>H<sub>2</sub> in absorption from diffuse gas, including two lines of sight in common with this work: NRAO150 (=B0355+508), and 3C111 (=B0415+379). The ambient hydrogen number densities they derived from a comparison of 18 and 21 GHz ortho- and para-absorption line strengths,  $n(\text{H}_2) = 2 \times 10^3 - 2 \times 10^4 \text{ cm}^{-3}$ , which were used in their excitation calculations, seem ruled out by the general weakness of mm-emission from species like HCO<sup>+</sup> and HCN (Lucas & Liszt 1996; Liszt 1997). Nonetheless, their column densities are in excellent agreement with ours. Their values are  $6.3 \times 10^{12} \text{ cm}^{-2}$  and  $4.8 \times 10^{12} \text{ cm}^{-2}$  for NRAO150 and 3C111, respectively, while ours ( $4/3 \times N(\text{C}_3\text{H}_2 - \text{o})$ ) are  $6.4 \times 10^{12} \text{ cm}^{-2}$  and  $4.3 \times 10^{12} \text{ cm}^{-2}$ .

Therefore, differences in quoted relative abundances must arise from normalization, *i.e.* the means used to estimate  $N(\text{H}_2)$ . For instance, toward 3C111, which we discussed at some length in Lucas & Liszt (1998) ( $N(\text{HCO}^+) \approx 1.2 \times 10^{13} \text{ cm}^{-2}$ ), Cox et al. (1988) used  $N(\text{H}_2) = 5 \times 10^{20}$ , implying a very high value for  $N(\text{HCO}^+)/(\text{H}_2) = 2.4 \times 10^{-8}$ . The extinction in this

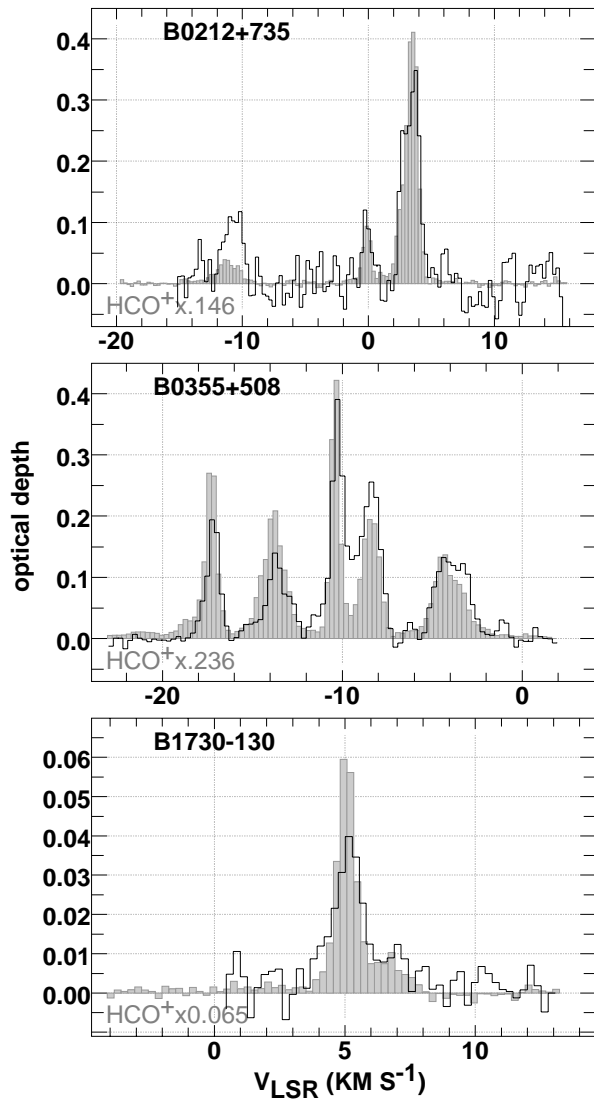


**Fig. 5.** Comparison of  $C_2H$  (lines) and  $HCO^+$  (shaded bars) spectra scaled to the area of the  $C_2H$  profile over various velocity ranges: at top, for  $v > -1 \text{ km s}^{-1}$ ; otherwise, over the whole profile.

direction is probably not less than 2 magnitudes, which is consistent with a relative abundance of  $HCO^+$  below about  $6 \times 10^{-9}$ .

#### 4.2. Relative abundances in diffuse, translucent, and dense clouds

Table 2 is a compilation of relative abundances covering diffuse and translucent clouds in the range  $A_V = 1$ -10 mag. The first column is a digest of species seen in optical and UV absorption toward  $\zeta$  Oph, mostly from the tables of Van Dishoeck & Black (1986); this line of sight has  $A_V = 1$  mag and the  $HCO^+$  column density is taken from the study of  $HCO^+$  emission by Liszt & Lucas (1994), for a density of  $n(H_2) = 200 \text{ cm}^{-3}$ . The column headed “This work” is meant to be representative of the present results. The column marked “TMC-1” contains entries from the compilation

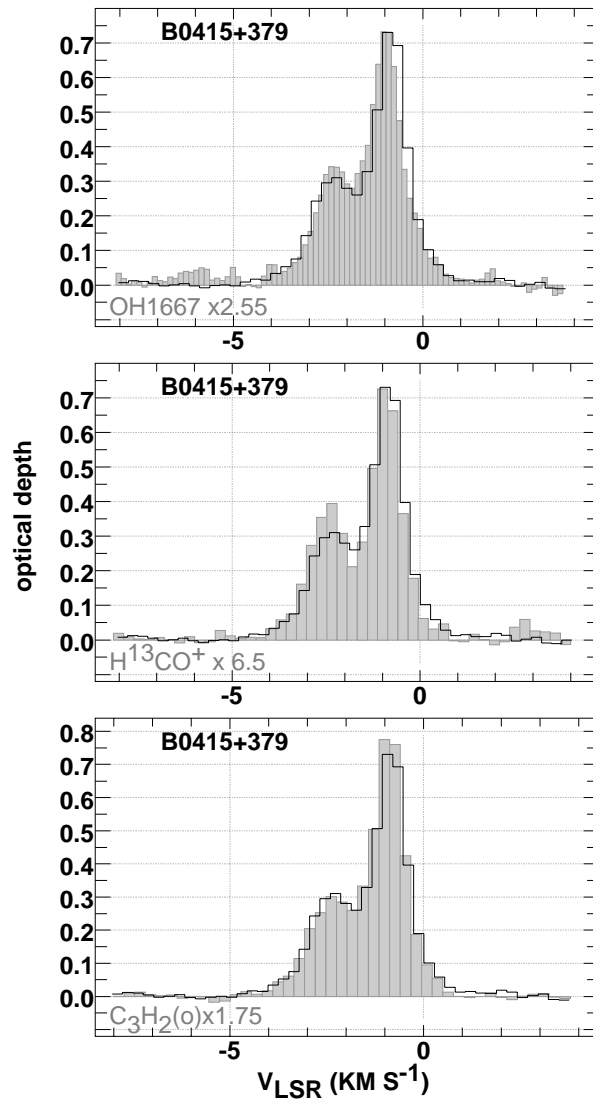


**Fig. 6.** Comparison of  $C_2H$  and other spectra (shaded) scaled to the area of the  $C_2H$  profile, toward B0415+379.

of Ohishi et al. (1992), which were normalized using  $N(H_2) = 10^{22} \text{ cm}^{-3}$  or just over 10 magnitudes of visual extinction. The last column shows the results of Model G of the  $\zeta$  Oph line of sight by Van Dishoeck & Black (1986), the most exhaustive study of quiescent, moderate-density, diffuse cloud chemistry.

Clearly, the abundances of many species – OH,  $HCO^+$  and  $C_2H$  – vary little from diffuse to dark gas: paradoxically, the seemingly ubiquitous species  $C_3H_2$  is not one of them. Instead, it, like  $C_3H$ , grows substantially more abundant in denser gas seen at higher extinction in dark clouds. By contrast, the abundance of CH probably declines by a small factor in denser material. An identical pattern,  $C_3/C_2 \ll 1$  and  $C_3H/C_2H \ll 1$  is repeated in diffuse gas and TMC-1. The abundances of species determined in emission are typically subject to uncertainties of factors of a few toward TMC-1 while the abundances seen in this work inherently vary by like amounts.

#### 4.3. The relative abundance of the linear and cyclic forms of $C_3H_2$

Cernicharo et al. (1999) recently detected linear  $C_3H_2$  ( $l-C_3H_2$ ) in absorption from the so-called spiral-arm clouds seen in absorption toward giant HII regions in the galactic plane (W49, W51, Sgr B2): we have also studied some of these sources, albeit for a very limited purpose; with reference mostly to SiO (Lucas & Liszt 2000). Cernicharo et al. (1999) find that the  $o-C_3H_2/l-C_3H_2$  ratio in the spiral-arm clouds, roughly 5, is an order of magnitude larger than what is found in dark clouds like TMC1 (where it is of order 50-100). The spiral-arm clouds have somewhat thicker gas columns than those seen in absorption toward our extragalactic sources, by factors of a few or more. For instance, at  $+39 \text{ km s}^{-1}$  toward W49, where  $N(o-C_3H_2) = 3.5 \times 10^{12} \text{ cm}^{-2}$  (some three times larger than any single feature seen here), our recent work (Lucas & Liszt 2000) showed  $N(HCO^+) \approx 60 N(H^{13}CO) = 1.9 \times 10^{13} \text{ cm}^{-2}$  or  $N(C_3H_2)/N(HCO^+) \approx 0.18$ , about a factor 4 higher than the mean for the clouds studied here. Apparently, the relative abundance of cyclic- $C_3H_2$  increases faster than that of linear- $C_3H_2$  during the transition from diffuse to darker material.

### 5. Diffuse cloud chemistry

Models of quiescent diffuse cloud gas-phase chemistry have their few possible successes – OH, CH,  $C_2$ , CN (see Table 2 and Federman et al. (1994)) – a couple of long-recognized failures ( $CH^+$ , CO) and a host of new problems like  $C_2H$ ,  $HCO^+$ ,  $H_2CO$ , and so on. The basic problem for the chemistry of trace species – how to get the ambient oxygen and carbon into molecular ions – is two-fold: atomic oxygen is only weakly ionized (by endothermic charge exchange with  $H^+$ ) and so does not participate in rapid ion-molecular hydrogen abstraction reactions ( $O^+ + H_2 \rightarrow OH^+ + H$ ), and the first ion of carbon unforgivably does not react rapidly with  $H_2$ . At thermal speeds, radiative association is slow and at thermal temperatures the endothermic hydrogen abstraction reaction ( $C^+ + H_2 \rightarrow CH^+ + H$ ) cannot proceed.

The outstanding failure of conventional models of quiescent diffuse cloud chemistry to reproduce the observed amounts of  $CH^+$  (by far the largest discrepancy in Table 2) led originally to the idea of  $CH^+$  formation in interstellar hydrodynamic shocks (Crutcher 1979; Elitzur & Watson 1980), which was subsequently generalized to a magnetohydrodynamic shock (Draine & Katz 1986) and serves as the basis for several other approaches.

The idea of models incorporating the interstellar magnetic field is to accelerate the dominant ionic species  $C^+$  and so drive the otherwise slow reactions of  $C^+$  and  $H_2$  (among other things) without overproducing OH and  $H_2O$ , as would occur if too much of the gas is heated (Falgarone et al. 1995; Federman et al. 1996). Bulk shock models fell from favor for nearly a decade, owing to several things; their prediction of velocity shifts, typically amounting to a few  $\text{km s}^{-1}$  between molecular ions ( $CH^+$ ) and other species, which were seldom

if ever observed; their seeming inability to produce  $N(CH^+)$  in excess of  $10^{13} \text{ cm}^{-2}$  per cloud; and the gradual emergence in the data of a correlation between  $N(CH^+)$  and reddening (Gredel et al. 1993). But they have recently been reexamined and shown to produce, of all things, the observed correlation between OH and  $HCO^+$  (Flower & Pineau Des Forêts 1998). Problems with predictions of unobserved kinematic differences between  $HCO^+$  and other species persist, however (Liszt & Lucas 2000), in these models.

In an effort to solve the  $CH^+$  problem without the problematic aspects of large-scale interstellar shocks, several proposals have been made to drive the  $C^+ + H_2$  reaction *in situ* in diffuse gas (Falgarone et al. 1995; Hogerheijde et al. 1995; Federman et al. 1996; Joulain et al. 1998), principally by the dissipation of turbulent (magnetic) energy. If this can be done, relatively large amounts of  $CH_2^+$  and  $CH_3^+$  can be sustained, and  $HCO^+$  can form from  $O + CH_3^+$  as well as from the reactions of  $C^+ + OH$  which dominate in quiescent cloud chemistries. It is claimed that the surprisingly high abundances we observe in diffuse gas can be explained in this way, although the similarity of dark cloud and diffuse gas relative abundance patterns seems a remarkable coincidence.

Most recently, Viti et al. (2000) have explored the possibility that  $C^+$  recombines on grains to form  $CH_4$ , which is then released into the gas phase and where its photodissociation products lead to enhanced abundances of simple hydrocarbons like  $C_2H$ , and to  $H_2CO$ , etc. Unfortunately, their results still do not produce sufficiently high abundances to explain our observations if the visual extinction is assumed to be as low as 1 mag.

The systematics of such turbulent chemistries remain to be explored but in the meantime we will produce a series of papers, beginning here, in which the systematics of several chemical groupings are exposed and compared. The next paper in this series will deal with cyanogen-bearing species such as HCN, HNC and CN. This will be followed by works discussing sulphur chemistry ( $CS$ ,  $SO$ ,  $SO_2$ ,  $H_2S$  and  $HCS^+$ ), and  $NH_3$  and  $H_2CO$ .

*Acknowledgements.* The National Radio Astronomy Observatory is operated by AUI, Inc. under a cooperative agreement with the US National Science Foundation. IRAM is operated by CNRS (France), the MPG (Germany) and the IGN (Spain). We owe the staff at IRAM (Grenoble) and the Plateau de Bure our thanks for their assistance in taking the data.

### Appendix A: products of gaussian fitting

See Tables A1 and A2.

### References

- Cardelli J. A., Mathis J. S., Ebbets D. C., Savage B. D., 1993, 402, L17
- Cernicharo J., Cox P., Fossé D., Güsten R., 1999, 351, 341
- Cox P., Guesten R., Henkel C., 1988, 206, 108
- Crutcher R. M., 1979, 231, L151
- Douglas A. E., Herzberg G., 1941, 94, 381
- Draine B. T., Katz N., 1986, 310, 392
- Elitzur M., Watson W. D., 1980, 236, 172

**Table A.1.** C<sub>2</sub>H Absorption line decomposition products

Source	$\nu$ km s <sup>-1</sup>	$\tau_0$	FWHM km s <sup>-1</sup>	$\int \tau d\nu$ km s <sup>-1</sup>	
B0212+735	-10.653(0.108)	0.103(0.011)	1.428(0.244)	0.378(0.077)	
	0.020(0.092)	0.089(0.015)	0.777(0.208)	0.177(0.056)	
	2.650(0.128)	0.134(0.020)	0.753(0.236)	0.259(0.091)	
	3.669(0.063)	0.387(0.015)	1.014(0.119)	1.002(0.124)	
B0224+671	-12.067(1.589)	0.026(0.006)	8.760(3.376)	0.592(0.267)	
	-10.492(0.131)	0.053(0.013)	1.163(0.368)	0.157(0.064)	
	-5.749(0.821)	0.020(0.012)	2.852(2.697)	0.148(0.169)	
	-1.953(0.146)	0.110(0.009)	2.786(0.528)	0.787(0.162)	
B0355+508	0.597(0.166)	0.049(0.014)	1.161(0.401)	0.144(0.066)	
	-17.140(0.019)	0.186(0.005)	0.914(0.041)	0.434(0.022)	
	-13.638(0.041)	0.118(0.003)	1.840(0.090)	0.554(0.031)	
	-10.200(0.012)	0.358(0.005)	0.916(0.026)	0.837(0.026)	
B0415+379	-8.423(0.019)	0.258(0.004)	1.335(0.044)	0.880(0.032)	
	-3.893(0.042)	0.130(0.003)	1.990(0.092)	0.662(0.035)	
	-2.234(0.016)	0.307(0.002)	1.671(0.032)	1.310(0.026)	
	-0.818(0.005)	0.664(0.004)	0.852(0.009)	1.447(0.019)	
B0528+134	-0.139(0.039)	0.091(0.003)	1.311(0.066)	0.305(0.019)	
	9.508(0.040)	0.165(0.011)	0.919(0.090)	0.387(0.046)	
	B0552+398	-16.136(0.063)	0.069(0.005)	1.509(0.143)	0.265(0.031)
	-4.682(0.053)	0.067(0.009)	0.821(0.123)	0.141(0.028)	
B0607-157	12.386(0.129)	0.023(0.003)	1.616(0.295)	0.095(0.021)	
B0736+017	6.606(0.035)	0.163(0.010)	0.967(0.079)	0.404(0.041)	
B0954+658	-19.256(0.075)	0.058(0.013)	0.526(0.179)	0.078(0.032)	
	4.001(0.025)	0.233(0.012)	0.813(0.056)	0.485(0.042)	
B1730-130	4.990(0.082)	0.042(0.003)	1.387(0.183)	0.150(0.022)	
	7.089(0.451)	0.009(0.002)	1.818(1.098)	0.040(0.027)	
B1741-038	0.252(0.775)	0.012(0.002)	5.292(1.828)	0.165(0.062)	
	4.074(0.070)	0.086(0.004)	1.871(0.180)	0.413(0.044)	
B1928+738	6.698(0.194)	0.034(0.003)	2.319(0.437)	0.201(0.041)	
	-2.244(0.229)	0.013(0.002)	2.425(0.533)	0.080(0.021)	
B1954+513	1.166(0.065)	0.118(0.014)	0.902(0.148)	0.273(0.055)	
B2037+511	-57.450(0.030)	0.138(0.007)	0.897(0.068)	0.316(0.029)	
	-10.740(0.100)	0.047(0.006)	1.245(0.229)	0.149(0.033)	
B2037+511	-57.456(0.029)	0.069(0.004)	0.849(0.066)	0.149(0.014)	
	-10.733(0.107)	0.021(0.003)	1.192(0.245)	0.065(0.016)	
B2145+067	-10.052(0.104)	0.015(0.004)	0.578(0.242)	0.022(0.012)	
B2200+420	-1.315(0.083)	0.451(0.076)	0.749(0.185)	0.864(0.260)	
	-0.537(0.091)	0.252(0.095)	0.442(0.265)	0.285(0.205)	
B2251+158	-10.107(0.111)	0.049(0.004)	1.941(0.252)	0.244(0.037)	

Falgarone E., Pineau Des Forêts G., Roueff E., 1995, 300, 870  
 Federman S. R., Rawlings J. M. C., Taylor S. D., Williams D. A., 1996, 279, L41  
 Federman S. R., Strom C. J., Lambert D. L., Cardelli J. A., Smith V. V., Joseph C. L., 1994, 424, 772  
 Flower D. R., Pineau Des Forêts G., 1998, 297, 1182  
 Gottlieb C. A., Gottlieb E. W., Thaddeus P., 1983a, 264, 740  
 Gottlieb C. A., Gottlieb E. W., Thaddeus P., Kawamura H., 1983b, 275, 916  
 Gottlieb C. A., Gottlieb E. W., Thaddeus P., Vrtilek J. M., 1986, 303, 446  
 Gredel R., Van Dishoeck E. F., Black J. H., 1993, 269, 477  
 Hogerheijde M. R., De Geus E. J., Spaans M., Van Langevelde H. J., Van Dishoeck E. F., 1995, 441, L93

**Table A.2.** ortho-C<sub>3</sub>H<sub>2</sub> Absorption line decomposition products

Source	$\nu$ km s <sup>-1</sup>	$\tau_0$	FWHM km s <sup>-1</sup>	$\int \tau d\nu$ km s <sup>-1</sup>
B0212+735	-11.353(0.098)	0.088(0.018)	1.008(0.228)	0.095(0.029)
	-0.781(0.110)	0.072(0.019)	0.853(0.256)	0.065(0.027)
B0355+508	2.956(0.054)	0.202(0.017)	1.417(0.124)	0.304(0.037)
	-17.263(0.044)	0.182(0.021)	0.799(0.100)	0.155(0.027)
B0415+379	-13.838(0.122)	0.071(0.017)	1.091(0.286)	0.083(0.029)
	-10.234(0.045)	0.244(0.018)	1.303(0.111)	0.338(0.038)
	-8.333(0.043)	0.225(0.020)	0.963(0.101)	0.230(0.032)
	-3.879(0.105)	0.119(0.013)	2.094(0.242)	0.265(0.042)
B0528+134	-2.277(0.030)	0.170(0.003)	1.680(0.061)	0.303(0.012)
	-0.875(0.008)	0.438(0.008)	0.866(0.021)	0.404(0.012)
B1730-130	0.114(0.055)	0.041(0.004)	0.667(0.112)	0.029(0.006)
	9.626(0.104)	0.063(0.018)	0.761(0.244)	0.051(0.022)
B2200+420	5.160(0.050)	0.041(0.003)	1.517(0.127)	0.066(0.007)
	6.837(0.068)	0.019(0.004)	0.579(0.160)	0.012(0.004)
B2200+420	-1.370(0.025)	0.146(0.010)	0.695(0.037)	0.108(0.010)
	-0.541(0.047)	0.119(0.004)	0.986(0.078)	0.125(0.011)
	1.558(0.086)	0.015(0.003)	0.908(0.204)	0.015(0.004)

Joulain K., Falgarone E., Des Forets G. P., Flower D., 1998, 340, 241  
 Liszt H. S., 1995, 442, 163  
 Liszt H. S., 1997, 322, 962  
 Liszt H. S., Lucas R., 1994, 431, L131  
 Liszt H. S., Lucas R., 1995, 299, 847  
 Liszt H. S., Lucas R., 1996, 314, 917  
 Liszt H. S., Lucas R., 2000, 355, 333  
 Lovas F. J., Suenram R. D., Ogata T., Yamamoto S., 1992, 399, 325  
 Lucas R., Liszt H., 1998, 337, 246  
 Lucas R., Liszt H. S., 1993, 276, L33  
 Lucas R., Liszt H. S., 1994, 282, L5  
 Lucas R., Liszt H. S., 1996, 307, 237  
 Lucas R., Liszt H. S., 1997, In: D. J. Jansen, M. R. Hogerheijde, E. F. Van Dishoeck (eds.), *Molecules in astrophysics: Probes and processes* (IAU Symposium 178, held in Leiden, The Netherlands, July 1-5, 1996), Leiden: Kluwer, p. 421  
 Lucas R., Liszt H. S., 2000, 355, 327  
 Marscher A. P., Bania T. M., Wang Z., 1991, 371, L77  
 Matthews H. E., Irvine W. M., 1985, 298, L61  
 Meyer D. M., Roth K. C., 1991, 376, L49  
 Ohishi M., Irvine W., Kaifu N., 1992, in P. D. Singh (ed.), *Astrochemistry of cosmic phenomena: proceedings of the 150th Symposium of the International Astronomical Union, held at Campos do Jordao, Sao Paulo, Brazil, August 5-9, 1991*. Dordrecht: Kluwer 1992, pp 171+  
 Swings P., Rosenfeld L., 1937, 86, 483  
 Thaddeus P., Gottlieb C. A., Hjalmarsen A., Johansson L. E. B., Irvine W. M., Friberg P., Linke R. A., 1985a, 294, L49  
 Thaddeus P., Vrtilek J. M., Gottlieb C. A., 1985b, 299, L63  
 Tucker K. D., Kutner M. L., Thaddeus P., 1974, 193, L115  
 Van Dishoeck E. F., Black J. H., 1986, 62, 109  
 Viti S., Williams D. A., O'Neill P. T., 2000, 354, 1062  
 Vrtilek J. M., Gottlieb C. A., Thaddeus P., 1987, 314, 716  
 Wooten A., Bozayan E. P., Garrett D. B., Loren R. B., Snell R. L., 1980, 239, 844